Thin Films of Octahedral Molecular Sieves of Manganese Oxide

Scott R. Segal,[†] Sang Hyun Park,[†] and Steven L. Suib*[,†,‡,§]

U-60, Department of Chemistry, Department of Chemical Engineering, and Institute of Materials Science, University of Connecticut, Storrs, Connecticut 06269-3060

Received April 3, 1996. Revised Manuscript Received September 3, 1996[⊗]

Octahedral layered molecular sieve materials (OL-1) having the birnessite structure have been synthesized using sol−gel preparation methods. The sol obtained by redox reaction between sucrose and $KMnO_4$ is then used to make films via (a) immersion, (b) spray coating, (c) spin coating, and (d) spatula coating. Crystalline OL-1 thin films have been prepared by methods a−c. Thin homogeneous films are most readily prepared by spray coating. Spin coating leads to noncrystalline and manganese-deficient films. The films have been characterized by X-ray diffraction, scanning electron microscopy, energy-dispersive X-ray analysis, and scanning Auger microscopy. The microscopy and Auger experiments show that there was no charging, implying these samples are good electrical conductors. The films are free from large amounts of impurity ions and carbonaceous deposits formed during the syntheses.

Introduction

Manganese oxides are important in areas such as preparation of electrolytic manganese oxide (deposition at electrode surfaces), dry cell batteries, ferrite production (magnetic applications), as components of oxidation catalysts, and for cross-linking of rubber.[1] Potential applications in separation science,[2] environmental catalysis,[3] and biological systems[4] may also be possible. Other possibilities include use as sensors,[5] as supports for metal clusters,[6] and in disposal of radioactive metal ions.[7]

Organic oxidations[8] with manganese oxide have focused on dehydrogenations (loss of H) and incorporation of electronegative species (O). The activity of manganese oxides depend on particle sizes, solvents, methods of preparation, and other factors.[8] MnO_2 is often used for oxidation of allylic and benzylic alcohols to aldehydes or ketones. In addition, amines can be converted to imines, thiols to disulfides, sulfides into sulfoxides, etc.[8] Manganese oxides have been reported to deposit on surfaces of bacteria and play a role in the decomposition of humic substances.[9] Natural manganese oxides systems have also been shown to decompose halogenated hydrocarbons.[10] Decomposition of H_2O_2 has also been catalyzed by MnO_2.[11]

Thin films of stoichiometric MnO_2 have recently been prepared by radiofrequency cathodic sputtering[12] and by thermal decomposition of nitrate precursors.[13] The RF sputtered films have very low resistivity (1.5 Ω cm) and are highly dependent on atmospheres used for preparation, storage, and treatment due to loss of oxygen and by contamination of sodium clusters.[12] The structures of these RF sputtered films were described as being nearly amorphous.[12] The thermally prepared MnO_2 films contain micropores in the range 0.1−100 nm that influence the resultant electrical properties.[13] Oxygen vacancies also readily form in these types of films. Surface films of manganese oxide known as desert varnish are also readily formed in nature,[14] presumably by bacteria that cause migration of manganese to the surface of sandstones and other rocks in both desert and arctic climate regions. These protective coatings drastically decrease surface erosion.

The reaction of $KMnO_4$ with simple sugars to form manganese oxide gels was first reported in the early 1900s.[24] However, these gels were poorly characterized. Recently, it was found that heating these gels to 400−450 °C for a few hours resulted in the formation of birnessite.[25] We have recently reported the synthesis of several octahedral molecular sieves (OMS) and octahedral layer (OL) materials which are mixed valent

[†] Department of Chemistry.
[‡] Department of Chemical Engineering.
[§] Institute of Materials Science.
* To whom correspondence should be addressed.
[⊗] Abstract published in *Advance ACS Abstracts,* November 1, 1996.

(1) Büchner, W.; Schliebs, R.; Winter, G.; Büchel, K. H. *Industrial Inorganic Chemistry*; VCH: Weinheim, 1989; pp 277−288.
(2) Fisher, S. J.; Alexander, R.; Kagi, R. I. *J. Chromatogr.* **1993**, *642*, 205−209.
(3) Bertino, D. J.; Zepp, R. G. *Environ. Sci. Technol.* **1991**, *25*, 1267−1273.
(4) (a) Koulougliotis, D. H.; Donald, J.; Brudvig, G. W. *J. Am. Chem. Soc.* **1992**, *114*, 8322−8323. (b) Libby, E.; McCusker, J. K.; Schmitt, E. A.; Folting, K.; Hendrickson, D. N.; Christou, G. *Inorg. Chem.* **1991**, *30*, 3486−3495.
(5) (a) Yan, Y. G.; Bein, T. *Chem. Mater.* **1993**, *5*, 905−907. (b) Trolier-McKinstry, S.; Newnham, R. E. *MRS Bull.* **1993**, *April*, 27−33. (c) Xu, C. N.; Miyazaki, K. *Sens. Act. B. Chem.* **1993**, *14*, 523−524.
(6) Sachtler, W. M. H. *Acc. Chem. Res.* **1993**, *26*, 383−387.
(7) (a) Naggar, I. M.; El-Asby, M. A.; Abdel-Hamid, M. M.; Aly, H. F. *Solv. Extr. Ion Exch.* **1993**, *11*, 521−540. (b) Mishra, S. P.; Tiwary, D. *J. Radioanal. Nucl. Chem.* **1993**, *170*, 133−141.
(8) (a) Hudlický, M. *Oxidations in Organic Chemistry*; ACS Monograph, *186*, 1990; ACS: Washington, DC; pp 33−34, 159−161, 240−261, 274−289. (b) Bielanski, A.; Haber, J. *Oxygen in Catalysis*; Marcel Dekker, Inc.: New York, 1991. (c) Kung, H. H. *Transition Metal Oxides, Surface Chemistry and Catalysis*; Elsevier: Amsterdam, 1989.
(9) Sunda, W. G.; Kieber, D. J. *Nature* **1994**, *367*, 62−64.
(10) Ulrich, H. J.; Stone, A. T. *Environ. Sci. Technol.* **1989**, *23*, 421−428.
(11) Jiang, S. P.; Ashton, W. R.; Tseung, A. C. C. *J. Catal.* **1991**, *131*, 88−93.
(12) Fau, P.; Bonino, J. P.; Rousset, A. *Appl. Surf. Sci.* **1994**, *78*, 203−210.
(13) Bayrachni, B.; Cheremskoy, P.; Gomozov, V.; Murovzev, L.; Skatkov, L. *Thin Solid Films* **1991**, *201*, L7−L8.
(14) Potter, R. M.; Rossman, G. R. *Am. Mineral.* **1979**, *64*, 1219−1226.

S0897-4756(96)00215-3 CCC: $14.00

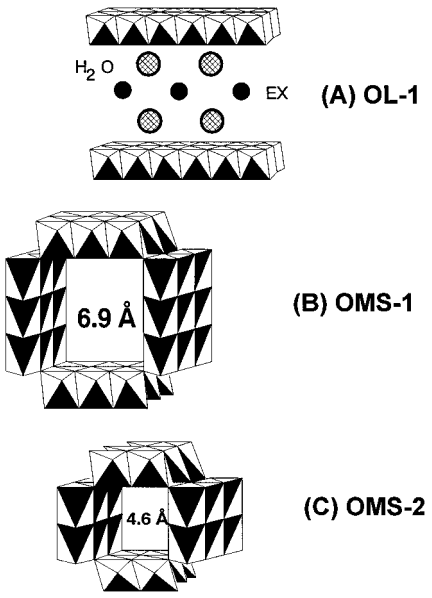

Figure 1. Structures of OMS and OL materials: (a) synthetic birnessite, (b) synthetic todorokite, and (c) synthetic cryptomelane.

manganese oxides.[15−21] OMS-1 is a tunnel structure system having a 1-dimensional tunnel with a 6.9 Å size which is similar to the mineral todorokite.[15,16] OMS-2 is a smaller size (4.6 Å) tunnel structure similar to that of the mineral cryptomelane.[17−19] OL-1 is a layered material with an interlayer spacing of about 7 Å which is similar to the mineral birnessite.[15−19] These synthetic manganese oxide mixed valent materials have interesting electrical,[15,16,19] magnetic,[18] photocatalytic,[20] surface,[21] and catalytic properties.[15,16] The conducting nature of these layer and tunnel structure materials sets them apart from most other molecular sieves.

The structures of OMS and OL materials are shown in Figure 1. The chemical formula for OL-1 is $(K,Na)_4Mn_{14}O_{27}\cdot 21H_2O$, for OMS-1 the formula is $Mg_{.1-1.4}{}^{II}Mn_{1.9}{}^{IV}Mn_{4.4-4.5}O_{12}\cdot 4.5H_2O$ and for OMS-2 the formula is $KMn_8O_{16}\cdot nH_2O$. The ability to prepare thin films of electrically conducting materials such as OMS and OL systems might allow further studies and applications in the fields of electrochemistry, sensors, batteries, adhesion, magnetics, catalysis, and other areas. The focus of research reported here has been to determine ideal methods for preparation of robust uniform thin films of OMS and OL materials. Thin films of OL-1 have been prepared with a variety of methods and have been characterized by X-ray powder diffraction, scanning electron microscopy, energy-dispersive X-ray analysis, and scanning Auger microscopy.

(15) Shen, Y. F.; Zerger, R. P.; DeGuzman, R. N.; Suib, S. L.; McCurdy, L.; Potter, D. I.; O'Young, C. L. *J. Chem. Soc., Chem. Commun.* **1992**, *17*, 1213−1214.
(16) Shen, Y. F.; Zerger, R. P.; DeGuzman, R. N.; Suib, S. L.; McCurdy, L.; Potter, D. I.; O'Young, C. L. *Science* **1993**, *260*, 511−515.
(17) DeGuzman, R. N.; Shen, Y. F.; Neth, E. J.; Suib, S. L.; O'Young, C. L.; Levine, S.; Newsam, J. M. *Chem. Mater.* **1994**, *6*, 815−821.
(18) Suib, S. L.; Iton, L. E. *Chem. Mater.* **1994**, *6*, 429−433.
(19) DeGuzman, R. N.; Shen, Y. F.; Suib, S. L.; Shaw, B. R.; O'Young, C. L. *Chem. Materials* **1993**, *5*, 1395−1400.
(20) Cao, H.; Suib, S. L. *J. Am. Chem. Soc.* **1994**, *116*, 5334−5342.
(21) Suib, S. L.; Cao, H.; Willis, W. S. In *Chemically Modified Surfaces*; Pesek, J. J., Leigh, I. E., Eds.; The Royal Society of Chemistry; London, 1994; pp 101−108.

Experimental Section

Preparation of Sol−Gel Materials. Gels were prepared by taking 0.73 M solutions of sucrose (J. T. Baker, Inc., Phillipsburg, NJ) prepared from 5.0 g of sucrose in distilled deionized water (DDW) and adding a 0.38 M solution of $KMnO_4$ prepared by dissolving 3.0 g of $KMnO_4$ (J. T. Baker, Inc., Phillipsburg, NJ) in 50 mL of DDW in a 150 mL beaker. The purple color of the $KMnO_4$ solution was retained after addition to the colorless sucrose solution. Reduction of $KMnO_4$ led to the formation of a brown, homogeneous sol which formed via an exothermic reaction while the mixture was stirred. After 15 min it solidified into a gel. Thin films were prepared by using both the sol and gel phases.

Preparation of Substrates. Copper metal foil (ALFA Ventron, Danvers, MA) and glass microscope slides (2.5 cm × 7.5 cm × 1 mm, Fisher Scientific, Pittsburgh, PA) were used as substrates for film deposition. Both the Cu and glass substrates were soaked in a solution of C_2H_5OH (AAPER Alcohol & Chemical Co., Shelbyville, KY)/KOH (J. T. Baker Chemical Co., Phillipsburg, NJ) for an hour to remove surface species. Etching of the Cu substrates was done according to literature procedures by placing concentrated HCl (J. T. Baker Chemical Co., Phillipsburg, NJ) over the foil while stirring for $^1/_2$ h at room temperature. Some Cu foils were further treated by washing with an aqueous solution of 1 M NaOH (Fisher Chemical Co., Fair Lawn, NJ) followed by rinsing with DDW. Substrates were sometimes etched instead with concentrated HNO_3. All substrates were dried at room temperature prior to film deposition.

Immersion Methods. After mixing the sucrose and $KMnO_4$ solutions, substrates were placed in the sol in a vertical orientation. Upon gelation, the beaker was transferred to an oven for drying at 110 °C for 24 h. The substrates were removed from the beaker and calcined in a furnace at temperatures between 300 and 450 °C for 2 h.

Spray Coating. In this method, N_2 gas was passed through a glass sprayer containing the sol. The sol was sprayed onto the substrates which in some cases were heated to high temperatures (300−350 °C) using a homemade glass sprayer. The distance from the sprayer to the substrate was approximately 30 cm. Single and multiple sweeps were sprayed over the surface. The pressure of the N_2 gas varied depending on the type of the sprayer and the viscosity of the sol. The lowest pressure at which the sol would exit the sprayer was generally used. The sol was allowed to mix for up to 10 min before being sprayed. Waiting longer than this period can lead to gelation inside the sprayer. After the substrate was coated, it was placed in an oven at 110 °C for 24 h and then calcined in the same manner described above for the immersion method.

Spin Coating. Manganese oxide sol was dropped continuously from a disposable pipet onto a rotating substrate. The total volume of sol was 1−2 mL for coatings on glass. Similar amounts of sol were used in proportion to the size of the Cu foils used for deposition on Cu substrates. After spin coating the coated substrates were dried in air at 110 °C for 24 h and calcined as described earlier.

There were four separate stages for preparation of spin-coated materials. The initial stage involved a low angular velocity ω_1 which led to deposition of a certain volume, v_1. The second developing stage was done with a medium angular velocity ω_2 and led to deposition of volume v_2. The third finishing stage was done after all sol was deposited on the surface and used a high angular velocity, ω_3. The final stage was an evaporation step which used the same angular velocity ω_3 as in the finishing stage. For these spin-coating experiments, $\omega_1 < \omega_2 < \omega_3$ and $v_1 < v_2$.

Spatula Coating. Thin layers of sol were coated onto glass and Cu substrates by spreading sol evenly onto the substrate with a stainless steel spatula. After deposition of the sol, it was air dried at 110 °C for 24 h and then calcined as described earlier.

X-ray Powder Diffraction. A Scintag Model PDS-2000 $\theta-\theta$ diffractometer was used for X-ray powder diffraction (XRD) experiments. Coated substrates were loaded directly onto the sample holder. Cu Kα radiation was used at 45 kV

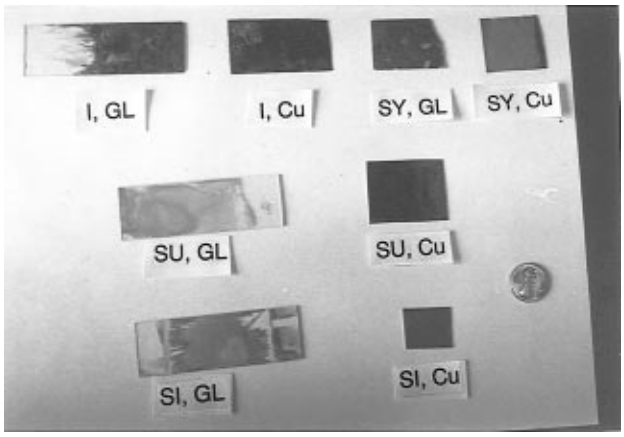

Figure 2. Photos of manganese oxide thin films on Cu or GL (glass) substrates prepared by various methods. I = immersion, SY = spray coating, SU = spatula coating, SI = spin coating.

and 40 mA. Sample scans were done at 5° 2θ/min. Thin-film experiments were done by replacing the collimator before the detector with a Scintag thin-film attachment.

Scanning Electron Microscopy/Energy-Dispersive X-ray Analysis. Scanning electron microscopy (SEM) and energy-dispersive X-ray (EDX) analyses were done on all of the thin-film samples. An Amray Model 1810 D SEM and an Amray Model PV 9800 EDX system were used. A beam voltage of 30 kV was typically used. Samples on Cu substrates were cut into 1 cm × 1 cm pieces and mounted onto a sample holder prior to analysis. Coated glass substrates were cut into small pieces (on the order of the Cu pieces mentioned above) for analysis.

Scanning Auger Microscopy. A Perkin-Elmer PHI Model 610 scanning Auger microprobe (SAM) with a cylindrical mirror analyzer was used for elemental analysis of the surface of the thin films. Depth profiles of the thin films were done by using argon ion sputtering of the surface of the thin films. An electron beam voltage of 3 kV primary beam energy was used and sample currents of 30 nA for the films coated on Cu substrates and 5 nA for thin films coated on glass were used. A lower beam current was used for the glass substrates due

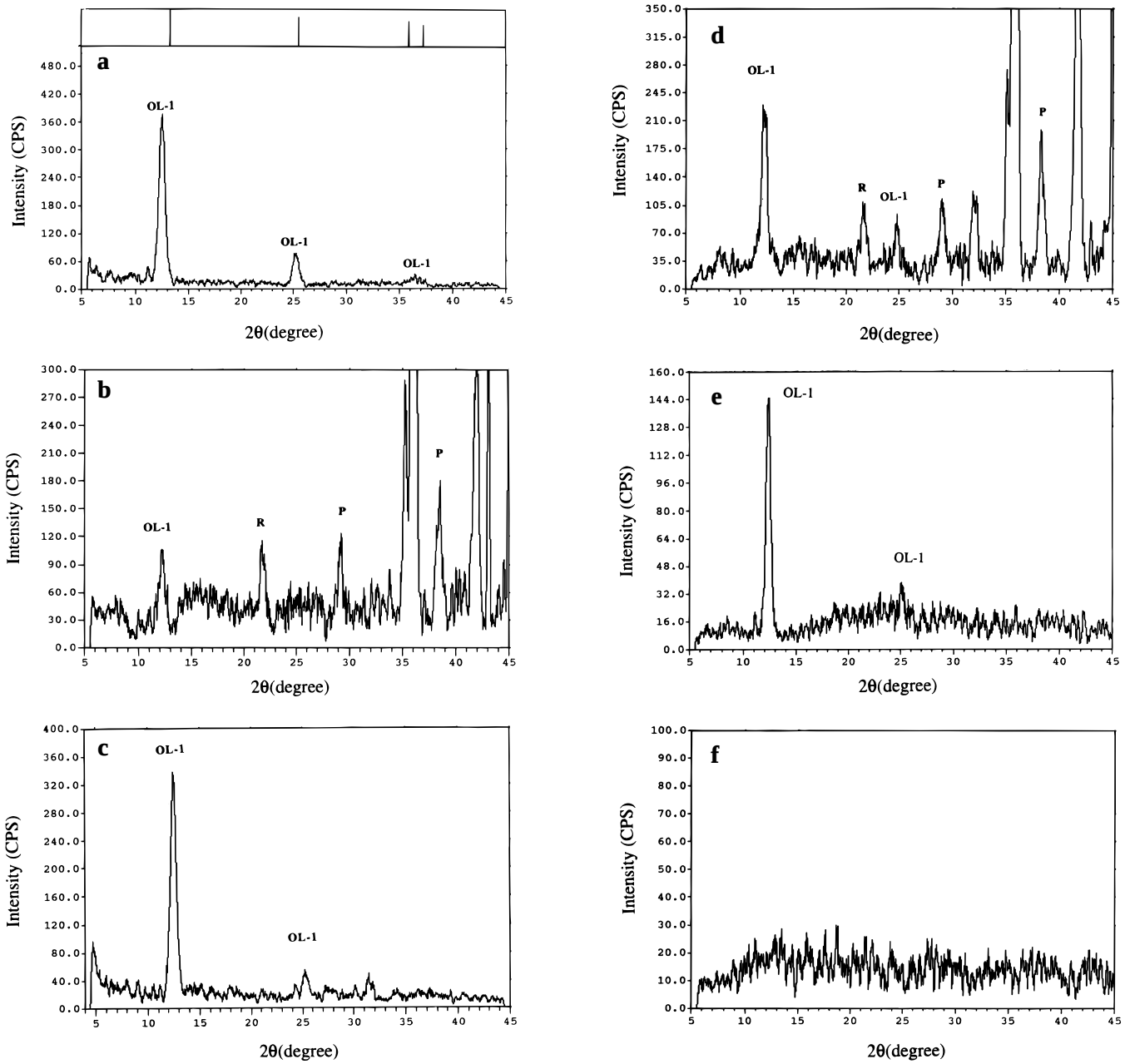

Figure 3. X-ray powder diffraction data for various methods and substrates: (a) immersion, glass with JCPDS pattern (23−1046) shown for birnessite, (b) immersion, Cu, (c) spray, glass, (d) spray, Cu, (e) spatula, glass, (f) spin, glass. OL-1 = birnessite, R = ramsdellite, P = pyrolusite.

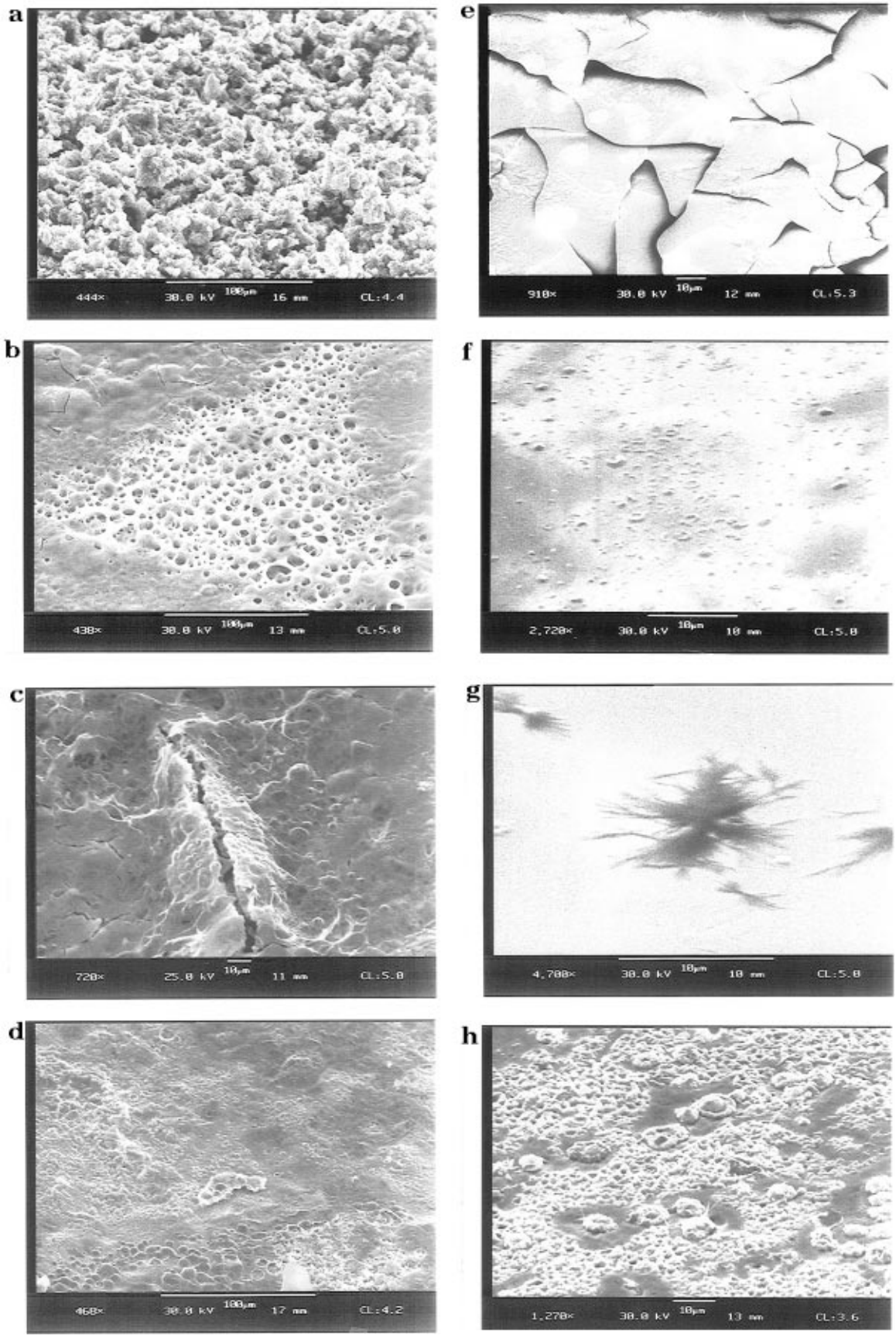

Figure 4. Scanning electron microscopy photos of thin films: (a) immersion, glass, (b) spray, glass, (c) spray, Cu, 1 h, (d) spray, Cu, 2 h, (e) spatula, glass, 250 °C, 4 h, (f) spin, glass, 350 °C, 4 h, (g) spin, glass, 250 °C, 6 h, (h) spin, Cu.

to surface charging problems. During data collection the pressure was maintained in the range of 1×10^{-10} Torr. A NECA PC was interfaced to the SAM and used for all data collection and analysis with software available from RBD Enterprises, (Eden Prairie, MN).

Results

A photo of the thin films of manganese oxide prepared by various methods on both Cu and glass substrates is shown in Figure 2. The spin coated films are so thin

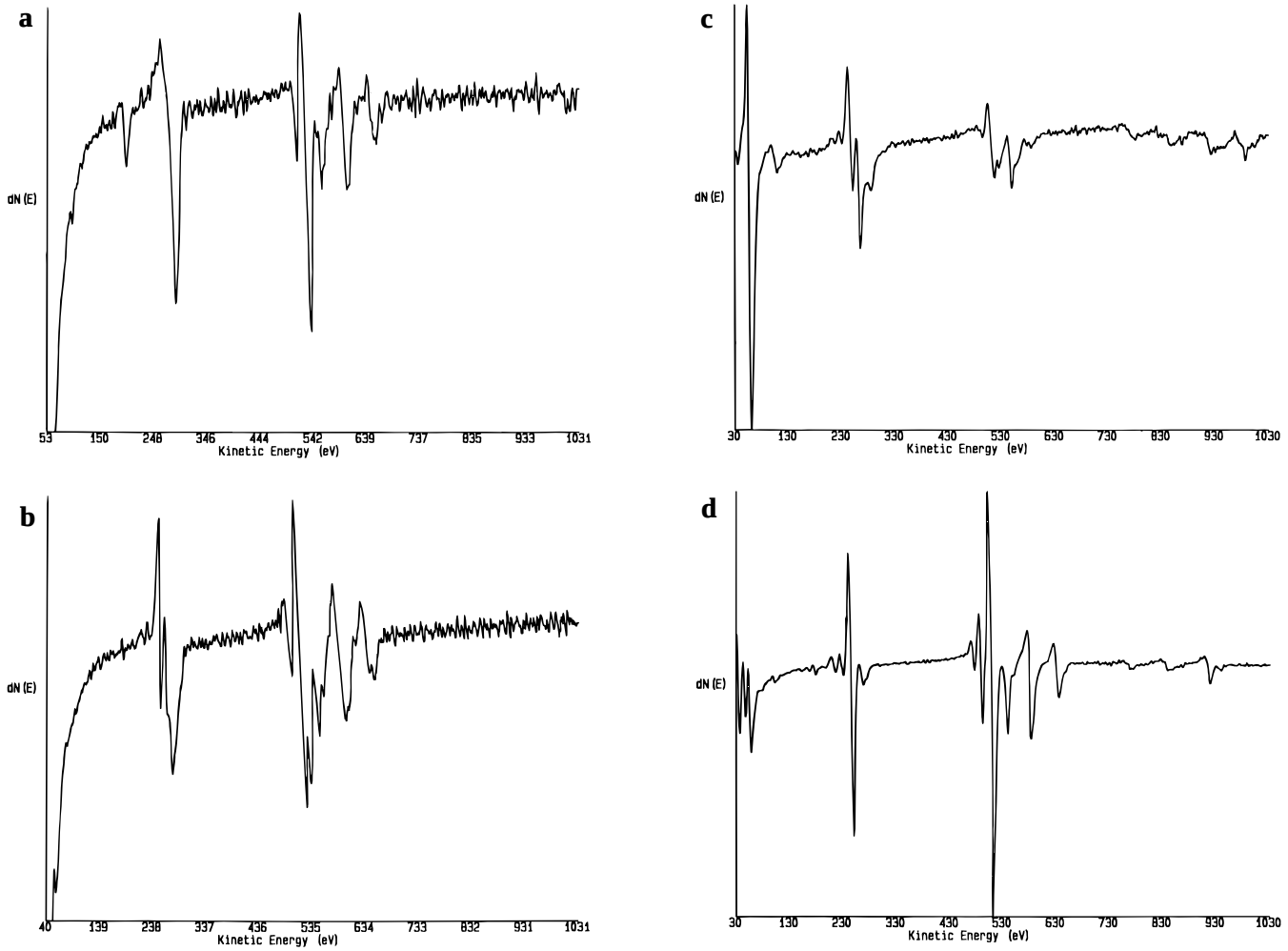

Figure 5. Scanning Auger microscopy data for thin films: (a) spin, glass, (b) spray, glass, (c) spin Cu, (d) spray, Cu.

Table 1. Energy-Dispersive X-ray Data for Thin Films

method	substrate	K/Mn
immersion	glass	0.7
spray coating	copper	1.5
spatula coating	glass	1.3

that they are not visible to the eye. The immersion coated films are relatively thick and are readily observable on both types of substrates.

Structural Studies. XRD data for manganese oxide thin films prepared by the immersion method on glass and on Cu substrates are shown in Figure 3a,b, respectively. Figure 3a shows data when the thin-film attachment was used, and peaks near 7.0 and 3.5 Å are readily observed for the glass substrate. Figure 3b shows XRD data for films prepared by immersion on Cu substrates. Peaks at 7.2, 4.1, and 3.0 Å are observed, with a variety of strong peaks between 35 and 45° 2θ, which are due to the Cu substrate. XRD data for spray coated films on glass with the thin film attachment are shown in Figure 3c, with peaks at 7.0 and 3.5 Å being observed. Corresponding XRD data for the spray coated material on Cu substrate are shown in Figure 3d with peaks at 7.1, 4.1, and 3.6 Å, as well as peaks for the Cu substrate between 35 and 45° 2θ.

XRD data for spatula coated thin films on glass are shown in Figure 3e. Peaks at 7.1, 3.5, and 2.5 Å are observed. Spin-coated materials on glass show no readily discernible powder diffraction peaks as shown in Figure 3f. XRD data for spin-coated materials on Cu substrates show strong peaks between 35 and 45° 2θ due to the Cu substrate as well as some broad diffraction peaks near 7.0 and 3.5 Å.

Scanning Electron Microscopy. SEM data for the thin films prepared by various methods are shown in Figure 4. Figure 4a shows a thin film prepared by the immersion method for a glass substrate. The particles are large with sizes ranging from 10 to 50 μm. A thick coating of particles is apparent. Figure 4b shows SEM data for films prepared by spray coating on a glass substrate which was preheated to 300 °C. Pinholes ranging from about 1 to about 5 mm are observed across the surface, although less porous coatings are observed in other areas (upper and lower left side of photo).

SEM data of Figure 4c show a spray-coated Cu substrate that had been etched with HCl. Microcracks are observed in many regions of the photo with one large crack shown in the middle. Figure 4d shows a spray-coated film on a Cu substrate that had been heated for 2 h. In this case a relatively uniform surface is observed with no apparent microcracks, although there is an unevenness to the surface deposition.

SEM photos for spatula coated films on glass calcined at 250 °C for 4 h are shown in Figure 4e. Interlocking flat films are observed in this photo. Figure 4f shows an SEM photo for a spin-coated film calcined at 350 °C for 4 h. There do not appear to be pinholes or cracks in these films, although particulates or blisters on the order of 1 μm are observed on the surface. For spin-coated samples calcined at 250 °C for 6 h, 10 μm star-shaped or snowflake-shaped features are observed

Table 2. Scanning Auger Microanalysis for Thin Films

method	substrate	peaks (eV)	assignment	K/Mn[a]
spin coating	glass	199	Cl	
		287	C,K	0.13
		532	O	
		556, 601, 659	Mn	
spray coating	glass	182	Cl	0.37
		256	K	
		274	C	
		513	O	
		541, 591, 647	Mn	
spin coating	copper	110	not assigned	0.01
		251	K	
		266	C	
		518	O	
		527, 550, 587	Mn	
		781, 849, 924	Cu	
		989	Na	
spray coating	copper	179	Cl	0.74
		250	K	
		268	C	
		513	O	
		540, 587, 637	Mn	
		772, 838, 907	Cu	

[a] Surface K/Mn ratios.

which appear to be voids below the surface of the film as shown in Figure 4g. For samples that were prepared by spin coating on Cu substrates, islands on the order of 5 μm were formed as shown in Figure 4h.

Energy-Dispersive X-ray Analyses. Semiquantitative K/Mn ratios for thin films prepared by immersion on glass, spray coating on Cu, and spin coating on glass are given in Table 1. The K/Mn ratios vary from 0.7 to 1.3. The EDX data are semiquantitative due to surface roughness of the particulates and are used here only to get a rough idea of the varying K and Mn concentrations in these materials.

Scanning Auger Microscopy. Figure 5a−d shows scanning Auger microscopy data for thin films that have been spin coated on glass, spray coated on glass, spin coated on Cu, and spray coated on Cu, respectively. Peak assignments and surface K/Mn ratios are given in Table 2.

Discussion

Structure. The X-ray powder diffraction data of Figure 3 clearly show diffraction peaks for most of these samples at 7.0 and 3.5 Å. These peaks are indicative of the octahedral layer phase OL-1, which has the birnessite structure.[15−19] The JCPDS pattern for birnessite is shown in Figure 3a. The peak at 7.0 Å belongs to the (002) reflection, with the peak at 3.5 Å belonging to the (212) reflection. Immersed glass samples show a small peak at 2.5 Å, which is also indicative of OL-1. This can be seen in Figure 3a.

The samples prepared by immersion and spray methods on Cu substrates (see Figure 3b,d) show a weak peak at 7.0 Å just like the much more intense peak for the glass substrate in Figure 3a. For immersed and sprayed Cu substrates, extra peaks which cannot be attributed to OL-1 or Cu appear at 4.1, 3.0, and 2.3 Å. The peak at 4.1 Å is indicative of ramsdellite, a 1 × 2 tunnel structure while the peaks at 3.0 and 2.3 Å may be due to pyrolusite. The immersed Cu substrate does not show a peak at 3.5 Å. This may be explained by noting that in other X-ray patterns, such as Figure 3a, the peak at 3.5 Å is about 30% as intense as the peak at 7.0 Å. If that lower percentage is applied to the 3.5 Å peak in Figure 3b, then the predicted intensity would be about 30 counts/s, which is at the level of noise of this pattern.

The glass coated materials show very clean XRD patterns that are readily indexed due to the amorphous nature of the glass. On the other hand, the Cu substrates show several extra diffraction peaks between 35 and 45° 2θ, which can be assigned to both Cu and CuO from the substrate.[22] The spin-coated materials do not show any diffraction peaks. These materials are very thin, on the order of 0.5 μm, and represent the thinnest of all the synthetic methods that were used.

The average crystallite size of the birnessite phase was determined using computer software provided with the X-ray diffractometer. This calculation is based on the Scherrer equation, relating peak broadening to crystallite size. The calculation was made using the (002) reflection for all the films. The average crystallite sizes ranged from about 110 to 150 Å. Similar calculations were performed on a birnessite material prepared by our group using a precipitation method.[16] The average crystallite size for this other material was 55 Å. This suggests that the sol−gel synthesis of birnessite produces slightly larger crystals than do precipitation methods.

Composition. The X-ray powder diffraction data of Figure 3 clearly show the formation of birnessite which is a mixed valent manganese oxide with K^+ counterions. The degree of K^+ substitution can vary depending on the method of preparation, the presence of other cations, and due to ion-exchange effects during synthesis or after synthesis.[15−19] The composition of OL-1 also can vary depending on the method of preparation, i.e., reflux, sol−gel, etc.[17,19] Bulk analyses of birnessite yield K/Mn ratios on the order of 0.5, which is close to the EDX determined value of 0.7 obtained for the sample prepared by immersion methods on a glass substrate. XRD data of Figure 3a suggest that crystalline OL-1 has been prepared with no evidence of other crystalline impurities, therefore supporting the EDX data.

On the other hand, the K/Mn ratios for the sprayed Cu material and the spatula-coated glass material are 1.5 and 1.3, respectively, which are considerably different than that formed in birnessite. Those data suggest that there is either an excess of K^+ or a deficit of Mn on the substrates for the spray and spatula preparations.

EDX data showed that absolute amounts of K^+ and Mn are much lower for the spin-coated materials than all the other preparations. This is again consistent with XRD data. A thin amorphous layer of manganese oxide would appear as very low concentration in an EDX experiment. The relative amounts of K^+ and Mn determined from surface analyses for the spin coated materials are also low, suggesting that both the surface and bulk have low concentrations of such elements.

The SAM data of Figure 5 are also in agreement with the suggestion that OL-1 films are formed with the four different preparation methods. Both spin-coating and spray-coating methods can lead to impurity surface concentrations of Cl^-.

The fact that K^+ and C overlap for the spin-coated material suggests that sizable amounts of carbon are formed during synthesis that are not readily removable during treatment, as opposed to the other three methods

(22) Davis, S. P.; Borgstedt, E. V. R.; Suib, S. L. *Chem. Mater.* **1990**, *2*, 712−719.

Table 3. Comparison of Preparation Methods for Manganese Oxide Thin Films

property	immersion	spray	spin	spatula
homogeneity	uneven, particulates	even	islands on Cu	even
crystallinity	excellent	Cu > glass	amorphous	good
K/Mn	lowest	intermediate	low	high
adhesion	glass > Cu	oriented on glass	glass > Cu	both OK
synth temp (°C)	300−350	300−350	250−250	250−250
thickness (μm)	≫1	<1	≪1	<1

where C from the sugar reagent appears to be readily removed. The spin-coated Cu material also shows a peak for Na^+, which is an impurity that could be introduced during pretreatment of substrates. Spray-coated surface K/Mn ratios show ratios smaller than 1, consistent with the formation of OL-1.[15−19]

Morphology. SEM data of Figure 4 show that the morphologies of resultant films are very different when different methods of preparation are used. A reviewer has suggested that morphology and cracks may be related more to thickness than the coating method. This may be the case; methods like immersion lead to thick films with large number of cracks. Methods like spray and spin coating lead to thinner, crack-free films. Therefore, it may be easier to prepare thin, uniform, crack-free films with methods such as spray and spin coating where the sol is readily spread out over the substrate surface.

Immersion methods lead to formation of large particulates of manganese oxide at the glass or Cu interface that are similar to bulk powder materials. Spatula coated films are less than 1 μm in thickness. Etching Cu with HNO_3 produced a more even coating than etching with HCl.

Multiple sweeps in the spray-coating method formed thicker coatings which were more even, whereas single-sweep samples formed thinner uneven coatings. Other important factors that control surface morphology and homogeneity include the flow rate of the exiting sol from the sprayer (which was minimized for best results) and the amount of time used in spraying the substrates. This time period was minimized (∼2 s) to obtain the thinnest coatings.

Islands of manganese oxide formed during spin coating such as those observed in Figure 4e and cracks and pinholes observed in Figure 4b,c with the spray method, are indicative of effects that occur during thermal treatment. Solvent removal during drying leads to such features in certain methods to a greater extent than others. With proper spraying conditions, these cracks and pinholes can be minimized as shown in Figure 4d.

Overview. A comparison of the properties of films prepared by various method is given in Table 3. The most homogeneous thin coatings are the spray coated materials. The spatula coated materials are also evenly coated but are relatively thick coatings. The immersion method generates particulates at the surface and generally uneven coatings. The crystallinity of the thickest coatings prepared by the immersion and spatula coating methods is very good.

Spray coating leads to more crystalline films on Cu, whereas spin coating leads to amorphous coatings. The K/Mn ratio is quite variable depending on the method of preparation. The immersion and spin coating materials have larger surface manganese concentrations than the spray- and spatula-coated materials.

In general, the manganese oxide films adhere better to glass than Cu. This is in marked contrast to zeolite films prepared in our labs.[22,23] In certain cases such as spray coating on glass, there may be an orientation effect. The ratios of the peaks at 7.0 Å/3.5 Å for sprayed glass films is 6.0, while the ratio for immersed glass films is 4.8. Note that the full widths at half maxima of the peaks for these two sets of data are similar, so a comparison of ratios (7.0 Å/3.5 Å) should be possible. These data may suggest a difference in orientation of OL-1 on glass substrates, depending on the method of preparation. The peak at 7.0 Å belongs to the (002) reflection, suggesting that preferred orientation of films on glass prepared by spray methods is occuring along the *c* axis. The thicknesses of the films are also very different depending on the method of coating. Spin-coating methods lead to the thinnest films, which have thicknesses on the order of 0.5 μm.

Finally, these films show good electrical conductivity on the basis of the absence of charging observed in both the SEM and SAM experiments as was also observed for bulk OMS and OL materials.[15−19] Probing various regions of the films with a volt−ohm meter also led to low resistivity measurements and information regarding the homogeneity of these films. Conductivity measurements of these films are an ongoing part of our research.

Conclusions

This work involves the sol−gel preparation of manganese oxide films having the OL-1 structure. To the best of our knowledge, films of this type have not been made before. We have shown here that thin films of OL-1 can be prepared with a variety of thin-film techniques including spray coating and spin coating. Immersion methods generally lead to thick films of OL-1. Under the conditions used here, it is clear that the layered OL-1 structure is preferred for deposition on Cu or glass substrates which may be due to the 2 dimensional nature of films. The homogeneity of such OL-1 films is markedly dependent on the method of preparation with spin- and spray-coating methods giving the most homogeneous films. Spin coating affords the thinnest films. We are continuing studies of these thin films materials in photocatalytic, sensor, electrochemical, and battery systems.

Acknowledgment. We acknowledge the support of the Office of Basic Energy Sciences, Division of Chemical Sciences of the Department of Energy for this research.

CM9602151

(23) Creasy, K.; Deng, Y. P.; Park, J.; Borgstedt, E.; Davis, S. P.; Suib, S. L.; Shaw, B. R. *Mater. Res. Soc.* **1991**, *233*, 157−167.
(24) Witzemann, E. J. *J. Am. Chem. Soc.* **1915**, *37*, 1079−1091.
(25) Ching, S.; Landrigan, J. A.; Jorgenson, M. L.; Duan, N.; Suib, S. L.; O'Young, C. L. *Chem. Mater.* **1995**, *7*, 1604−1606.